ORIGINAL ARTICLE

Therapeutic Targeting of Vascular Remodeling and Right Heart Failure in Pulmonary Arterial Hypertension with a HIF-2α Inhibitor

Zhiyu Dai[1,2,3,4], Maggie M. Zhu[1,2,3,4], Yi Peng[1,2,3,4], Narsa Machireddy[1,2,3,4], Colin E. Evans[1,2,3,4], Roberto Machado[5], Xianming Zhang[1,2,3,4], and You-Yang Zhao[1,2,3,4,6,7]

[1]Program for Lung and Vascular Biology, Stanley Manne Children's Research Institute, Ann & Robert H. Lurie Children's Hospital of Chicago, Chicago, Illinois; [2]Division of Critical Care, Department of Pediatrics, Northwestern University Feinberg School of Medicine, Chicago, Illinois; [3]Department of Pharmacology and [4]Center for Lung and Vascular Biology, University of Illinois College of Medicine, Chicago, Illinois; [5]Division of Pulmonary, Critical Care, Sleep, and Occupational Medicine, Department of Medicine, Indiana University School of Medicine, Indianapolis, Indiana; and [6]Department of Pharmacology and Department of Medicine and [7]Feinberg Cardiovascular Research Institute, Northwestern University Feinberg School of Medicine, Chicago, Illinois

ORCID ID: 0000-0002-2945-7923 (Z.D.).

Abstract

Rationale: Pulmonary arterial hypertension (PAH) is a devastating disease characterized by progressive vasoconstriction and obliterative vascular remodeling that leads to right heart failure (RHF) and death. Current therapies do not target vascular remodeling and RHF, and result in only modest improvement of morbidity and mortality.

Objectives: To determine whether targeting HIF-2α (hypoxia-inducible factor-2α) with a HIF-2α–selective inhibitor could reverse PAH and RHF in various rodent PAH models.

Methods: HIF-2α and its downstream genes were evaluated in lung samples and pulmonary arterial endothelial cells and smooth muscle cells from patients with idiopathic PAH as well as various rodent PAH models. A HIF-2α–selective inhibitor was used in human lung microvascular endothelial cells and in *Egln1*^{Tie2Cre} mice, and in Sugen 5416/hypoxia- or monocrotaline-exposed rats.

Measurements and Main Results: Upregulation of HIF-2α and its target genes was observed in lung tissues and isolated pulmonary arterial endothelial cells from patients with idiopathic PAH and three distinct rodent PAH models. Pharmacological inhibition of HIF-2α by the HIF-2α translation inhibitor C76 (compound 76) reduced right ventricular systolic pressure and right ventricular hypertrophy and inhibited RHF and fibrosis as well as obliterative pulmonary vascular remodeling in *Egln1*^{Tie2Cre} mice and Sugen 5416/hypoxia PAH rats. Treatment of monocrotaline-exposed PAH rats with C76 also reversed right ventricular systolic pressure, right ventricular hypertrophy, and pulmonary vascular remodeling; prevented RHF; and promoted survival.

Conclusions: These findings demonstrate that pharmacological inhibition of HIF-2α is a promising novel therapeutic strategy for the treatment of severe vascular remodeling and right heart failure in patients with PAH.

Keywords: cardiac fibrosis; hypoxia-inducible factor; obliterative vascular remodeling; pulmonary arterial hypertension; pharmacological therapy

Pulmonary arterial hypertension (PAH) is characterized by excessive vasoconstriction and obliterative vascular remodeling that leads to right heart failure (RHF) and death (1–3). The histopathological features of PAH include thickening of the medial and adventitial layers of pulmonary vasculature, and the formation of vascular occlusions and plexiform lesions (4–6). Although significant advances have been made in understanding the pathogenesis of PAH, no effective therapy has been developed to

(Received in original form October 19, 2018; accepted in final form June 20, 2018)

Supported in part by NIH grants R01HL123957, R01HL125350, R01HL133951, and P01HL077806 (Project 3) to Y.-Y.Z. and K99HL138278 to Z.D.

Author Contributions: Z.D., R.M., and Y.-Y.Z. conceived the experiments. Z.D., M.M.Z., Y.P., N.M., C.E.E., and X.Z. designed and performed experiments, and analyzed the data. Z.D. and Y.-Y.Z. analyzed and interpreted the data. Z.D. wrote the manuscript. C.E.E. edited the manuscript. Y.-Y.Z. supervised the project and revised the manuscript.

Correspondence and requests for reprints should be addressed to You-Yang Zhao, Ph.D., Program for Lung and Vascular Biology, Stanley Manne Children's Research Institute, Ann & Robert H. Lurie Children's Hospital of Chicago, and Department of Pediatrics, Northwestern University Feinberg School of Medicine, 2430 N. Halsted Street, Box 220, Chicago, IL 60614. E-mail: youyang.zhao@northwestern.edu.

This article has an online supplement, which is accessible from this issue's table of contents at www.atsjournals.org.

Am J Respir Crit Care Med Vol 198, Iss 11, pp 1423–1434, Dec 1, 2018

Originally Published in Press as DOI: 10.1164/rccm.201710-2079OC on June 20, 2018
Internet address: www.atsjournals.org

At a Glance Commentary

Scientific Knowledge on the Subject: Previous studies demonstrated that HIF-2α (hypoxia-inducible factor-2α) activation secondary to PHD2 (prolyl hydroxylase-2) deficiency is obligatory to obliterative pulmonary vascular remodeling in mice. Mice with genetic ablation of HIF-2α are resistant to PHD2 deficiency or hypoxia-induced pulmonary arterial hypertension (PAH), but it is unknown whether a HIF-2α–selective inhibitor might be effective in the treatment of PAH in preclinical distinct animal models.

What This Study Adds to the Field: Our study found that targeting HIF-2α with a HIF-2α–selective inhibitor reverses established PAH, inhibits vascular remodeling and right heart failure, and promotes survival in rodent models. Thus, pharmacological inhibition of HIF-2α is a potentially effective approach for the treatment of PAH in patients.

reverse pulmonary vascular remodeling, inhibit RHF, and promote survival of patients with PAH. Current therapies mainly target the abnormalities in vasoconstriction in the prostacyclin, nitric oxide and endothelin signaling pathways, but not the obliterative vascular remodeling abnormalities. Hence, only modest improvements are achieved in PAH morbidity and mortality (7, 8). Therefore, novel therapeutic agents are urgently needed for patients with PAH.

Both HIF-1α (hypoxia-inducible factor-1α) and HIF-2α are important regulators of the response to hypoxia in the pulmonary circulation (9, 10). It has been demonstrated that both *Hif1a*$^{+/-}$ and *Hif2a*$^{+/-}$ mice exhibit blunted increases in right ventricular systolic pressure (RVSP) and RV hypertrophy in response to chronic hypoxia (11, 12). Ball and colleagues showed that genetic deletion of *Hif1α* in smooth muscle cells (SMCs) in mice attenuated RVSP and pulmonary arterial wall thickness in response to chronic hypoxia treatment (13). Intriguingly, RV remodeling was not affected in this model (13). *HIF2A* gain-of-function mutation is associated with severe PAH in patients (14). Mice with genetic knock-in of an activation mutation (G536W) of *Hif2a* also develop severe pulmonary hypertension (PH) (15). Studies have highlighted the predominant role of HIF-2α versus HIF-1α activation in the pathogenesis of PAH (16–19). Humans and mice with a *VHL* (von Hippel-Lindau) gain-of-function mutation develop PH (16, 20), whereas *Vhl*^{R200W} mice are rescued by heterozygous deletion of *Hif2a* but not *Hif1a* (16). Several groups including us demonstrated the critical role of endothelial HIF-2α but not HIF-1α activation in mediating pulmonary vascular remodeling and PH (17–19). Notably, HIF-2α activation secondary to HIF PHD2 (prolyl hydroxylase-2) deficiency in mice (*Egln1*^{Tie2Cre}) induced spontaneously obliterative vascular remodeling, severe PAH, and RHF, which resembles many pathological features of clinical PAH (17, 21, 22). Other groups showed that mice lacking HIF-2α but not HIF-1α in lung endothelium were resistant to hypoxia-induced PH (19). Taken together, these studies suggest that HIF signaling, specifically the PHD2/VHL/HIF-2α axis, is critical in regulating pulmonary vascular homeostasis.

Here we sought to determine the translational potential of targeting HIF-2α for the treatment of PAH and RHF, using a selective HIF-2α inhibitor. To the best of our knowledge, this is the first study showing that pharmacological treatment can effectively inhibit obliterative pulmonary vascular remodeling and RHF in three distinct rodent models of severe PAH. We also for the first time observed clear survival benefits in two of the three models through HIF-2α inhibition. Some of the results of these studies have been previously reported in the form of abstracts (23, 24).

Methods

Human Samples

Human lung tissues were obtained from patients undergoing lung transplantation for idiopathic pulmonary arterial hypertension (IPAH) and from unused donor lungs. Informed consent from patients and local ethics approval from the ethics committees of the Hammersmith Hospitals (reference No. 2001/6003) and Royal Brompton and Harefield Hospitals (reference No. 01-210) (London, UK) were obtained before tissue collection (17, 25, 26). Human IPAH pulmonary arterial endothelial cells (PAECs) and pulmonary arterial smooth muscle cells (PASMCs) were provided by R. Machado and the Pulmonary Hypertension Breakthrough Initiative (26).

Animals

All animal protocols were conducted according to National Institutes of Health guidelines on the use of laboratory animals. The animal care and study protocols were approved by the Institutional Animal Care and Use Committees of the University of Illinois at Chicago and Northwestern University.

Mouse model of PAH. *Egln1*^{Tie2Cre} mice at the age of 3 weeks were treated with vehicle (0.5% DMSO diluted in *N*-2-hydroxyethylpiperazine-*N*′-ethane sulfonic acid [HEPES] buffer) or C76 (compound 76) (12.5 mg/kg body weight, i.p., daily) for 12 weeks. C76 was dissolved in DMSO and diluted with HEPES buffer before injection. Both male and female mice were used.

Sugen 5416/hypoxia rat model of PAH. Male Sprague Dawley rats (Charles River Laboratories) at the age of 8 weeks were injected with Sugen 5416 (20 mg/kg body weight, subcutaneous, dissolved in DMSO) (Cat. No. 13342; Cayman) and then kept in a hypoxia chamber (BioSpherix) at 10% O_2 for 21 days. After a recovery period in normoxia (21% O_2) for another 21 days, all rats were randomly assigned to treatment with vehicle or C76 (12.5 mg/kg body weight, i.p.) daily for the subsequent 21 days. All rats were analyzed by echocardiography and hemodynamic measurements at 17 weeks old.

Monocrotaline rat model of PAH. Male Sprague Dawley rats at the age of 6 weeks were challenged with monocrotaline (MCT) (subcutaneous, 32 mg/kg body weight). Fourteen days after MCT treatment, rats were randomized to receive C76 (12.5 mg/kg, i.p., daily) or vehicle (0.5% DMSO) for 14 days. Echocardiography was performed, and RV hemodynamics were assessed before tissue collection 28 days after MCT treatment. For the survival study, rats were challenged with MCT at 35 mg/kg body weight.

Echocardiography and RV Hemodynamic Measurements

Echocardiography was performed with a Vevo 2100 ultrasound machine (FujiFilm

VisualSonics Inc) in the Cardiovascular Physiology Core of the Chicago Research Resources Center at the University of Illinois (17, 26, 27). RVSP was measured with a 1.4F (mice) or 3.5F (rats) pressure transducer catheter (Millar Instruments) as described previously (17, 25–27).

Human PASMC Proliferation Analysis

Human lung microvascular endothelial cells (HLMVECs) were transfected with scrambled siRNA or siRNA against PHD2, using an HMVEC-L Nucleofector kit with the Amaxa Nucleofector 2D device as described previously (17). Forty-eight hours after transfection, HLMVECs were incubated with DMSO or C76 (20 μM) in serum-free medium for another 24 hours. Conditioned medium was collected and added to serum-starved SMCs for 16 hours. 5-Bromo-2′-deoxyuridine (BrdU, 10 μM; Sigma) was added for incubation of SMCs with EC-conditioned medium. SMCs were immunostained with anti-BrdU–FITC (BD Biosciences) according to the manufacturer's instructions, and nuclei were counterstained with DAPI.

Luciferase Assays

HLMVECs were transfected with an HRE-Luc plasmid (Promega), or as an internal control pRL-TK plasmid, using an HMVEC-L Nucleofector kit with the Amaxa Nucleofector 2D device as described previously (17). To activate HIF-α, cells were treated with either dimethyloxallyl glycine (DMOG, 1 mM) or cotransfected with PHD2 siRNA. For the DMOG treatment study, the cells were treated with either DMSO, HIF-2α antagonist 2 (H2A, 20 μM), or HIF-2α translation inhibitor C76 (20 μM) for 24 hours. Both firefly and *Renilla* luciferase activities were assessed. The values are expressed as fold change relative to the DMSO group. For the PHD2 siRNA study, at 6 hours after transfection, the cells were treated with either DMSO, H2A (20 μM), or C76 (20 μM) for 14 hours and then assessed for firefly and *Renilla* luciferase activities.

Western Blotting Analysis

Western blotting analysis was performed with anti-PHD2 (diluted 1:2000) (Cat. No. 4835; Cell Signaling Technology), anti–HIF-1α (diluted 1:1000) (Cat. No. NB100-479; Novus Biologicals), or anti–HIF-2α antibodies (diluted 1:500) (Cat. No. NB100-122; Novus Biologicals). Anti–β-actin antibody (diluted 1:10,000) (Cat. No. A2228; Sigma-Aldrich) was used as a loading control.

Immunofluorescence Staining and Histological Assessment

Tissue processing and immunofluorescence staining were performed as described previously (17, 26). For histological assessment, sections were stained with a Russell-Movat pentachrome staining kit (American MasterTech) or with a trichrome stain (Masson) kit (Sigma-Aldrich) according to the manufacturer's instructions (17). Sections were imaged with an Aperio CS2 light microscope (Leica Biosystems).

Statistical Analysis

Statistical analysis of data was done with Prism 7 (GraphPad Software, Inc.). Statistical significance for multiple-group comparisons was determined by one-way ANOVA with Tukey *post hoc* analysis that calculates corrected P values. Two-group comparisons were analyzed by the unpaired two-tailed Student t test for equal variance or by Mann-Whitney test for unequal variance. Statistical analysis for the mortality study was assessed by the log-rank (Mantel-Cox) test. $P < 0.05$ denoted the presence of a statistically significant difference. All bar graphs represent means ± SD. Bars in dot plot figures represent the mean.

Detailed materials and methods are available in the online supplement.

Results

Activation of HIF-2α in Patients with IPAH and Three PAH Rodent Models

We first determined whether HIF-2α signaling is activated in lung tissues of patients with IPAH. Quantitative RT-PCR analysis showed that *HIF2A* but not *HIF1A* and HIF-2α downstream genes were upregulated in lung tissues from patients with IPAH compared with healthy donors (Figure 1A; *see* Figure E1A in the online supplement). Immunostaining demonstrated that upregulation of HIF-2α was located mainly in endothelial cells (ECs) of lung sections from patients with IPAH (Figure 1B) whereas HIF-1α was in SMCs (Figure E1B). Western blotting also showed that HIF-2α protein expression was highly induced in PAECs but not in PASMCs isolated from patients with IPAH (Figure 1C).

We next evaluated whether HIF-2α signaling is also induced in rodent models of severe PAH (Sugen 5416/hypoxia [SuHx]-treated rats, monocrotaline [MCT]-challenged rats, and $Egln1^{Tie2Cre}$ mice [28, 29]). We observed a marked increase in HIF-2α protein levels and its downstream target genes such as *Cxcl12* and *Il6* in the lungs of SuHx and MCT rats (Figures 1D, 1E, E2A, and E2B). Moreover, the expression of many HIF-2α genes was markedly increased in $Egln1^{Tie2Cre}$ mouse lungs, while attenuated or completely normalized in the lungs of $Egln1^{Tie2Cre}$/$Hif2a^{Tie2Cre}$ double-knockout mice (Figure E2C) but not in $Egln1^{Tie2Cre}$/$Hif1a^{Tie2Cre}$ double-knockout mice (data not shown), demonstrating the reliance of expression of these genes on HIF-2α activation. Together, these data demonstrate HIF-2α activation in lung tissues of three distinct rodent PAH models, as seen in patients with IPAH.

C76 Represses HIF-2α Activation in Human Lung Microvascular Endothelial Cells

To identify a potent HIF-2α–selective inhibitor in ECs, human lung microvascular ECs (HLMVECs) were transfected with HRE (hypoxia response element)–luciferase reporter plasmid, followed by treatment with H2A (HIF-2α antagonist 2) (30) or the HIF-2α–selective translation inhibitor C76 (31). Although both H2A and C76 reduced HRE–luciferase activity induced by PHD2 deficiency or DMOG treatment, C76 exhibited a more potent inhibitory effect than H2A (Figures 2A and E3A). Thus, we further characterized the impact of C76 treatment on HLMVECs. We observed marked inhibition of protein expression of HIF-2α but not HIF-1α in PHD2-deficient ECs and in DMOG-treated ECs after C76 treatment (Figures 2B and E3B), along with suppressed expression of HIF-2α target genes (Figure 2C). Our previous study demonstrated that one of the mechanisms of HIF-2α activation in PAH is the paracrine effect of dysfunctional ECs on promoting PASMC proliferation (17). Thus, we determined the effect of C76 on PHD2-deficient EC–induced PASMC proliferation. As shown in Figures 2D, 2E, and E3C, C76 treatment also inhibited the paracrine effect of PHD2-deficient ECs on

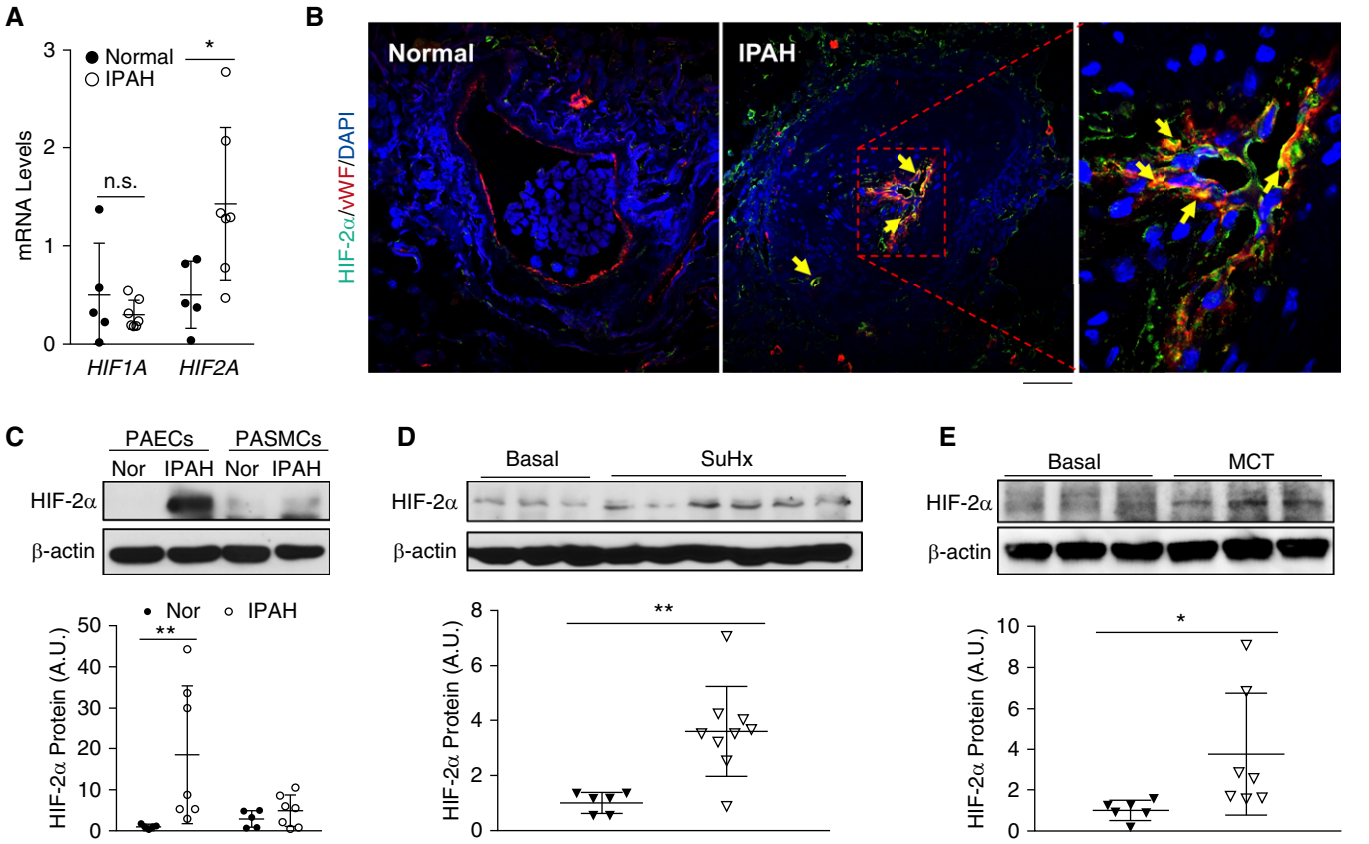

Figure 1. Activation of HIF-2α (hypoxia-inducible factor-2α) signaling in lungs from patients with idiopathic pulmonary arterial hypertension (IPAH) and rodent PAH models. (*A*) Quantitative RT-PCR analysis showing increase in *HIF2A* but not *HIF1A* expression in the whole lungs of patients with IPAH compared with healthy donors. (*B*) Immunofluorescence staining against HIF-2α demonstrating upregulation of HIF-2α expression predominantly in endothelial cells (ECs) (vWF^{+}). Arrows indicate HIF-2α (green)–positive ECs (red). Five normal donors and five patients with IPAH lung samples were analyzed. (*C*) Western blotting analysis demonstrating upregulation of HIF-2α in pulmonary arterial ECs (PAECs) but not pulmonary arterial smooth muscle cells (PASMCs) isolated from patients with IPAH compared with healthy donors. (*D*) Upregulation of HIF-2α protein levels in lungs from Sugen 5416/hypoxia (SuHx) rats compared with age- and sex-matched controls. Lung tissues from SuHx rats were collected 6 weeks after the 3-week SuHx challenge. (*E*) Increase in HIF-2α protein levels in lungs of monocrotaline (MCT)-exposed rats compared with controls. Lung tissues from MCT rats were collected 4 weeks after MCT exposure. Bars represent mean values. *$P < 0.05$ and **$P < 0.01$. (*A* and *C–E*) Mann-Whitney test. (*B*) Scale bar: 50 μm. A.U. = arbitrary units; Nor = normal healthy donors; n.s. = not significant; vWF = von Willebrand factor.

the proliferation of human PASMCs isolated from healthy donors and patients with IPAH. However, direct treatment of IPAH PASMCs with C76 affected neither proliferation nor apoptosis (Figures E3D and E3E).

Pharmacological Inhibition of HIF-2α Inhibits Obliterative Vascular Remodeling and Right Heart Failure in *Egln1*^{Tie2Cre} Mice

To assess the potential of targeting HIF-2α signaling for PAH treatment, we treated 3-week-old *Egln1*^{Tie2Cre} mice (with established PAH) (17) with C76 for 12 weeks (12.5 mg/kg, i.p., daily). C76 treatment resulted in marked reduction of HIF-2α but not HIF-1α protein levels and expression of HIF-2α downstream targets CXCL12 (C-X-C motif chemokine 12) and ET-1 (endothelin-1) in ECs from *Egln1*^{Tie2Cre} mice (Figures E4A–E4C), demonstrating the *in vivo* efficacy of C76 in inhibiting HIF-2α. As shown in Figure 3, C76 treatment resulted in marked reduction of RVSP (Figure 3A) and normalization of the PA acceleration time/ejection time (AT/ET) ratio, indicative of preserved PA function in *Egln1*^{Tie2Cre} mice (Figures 3B and 3C). In addition to hemodynamic improvement, C76 treatment also inhibited obliterative pulmonary vascular remodeling including lack of formation of neointima and vascular occlusive lesions, reduced pulmonary vascular wall thickness, and decreased muscularization of distal PAs (Figures 3D, 3E, E5A, and E5B). We also observed that C76 treatment reduced abnormal EC proliferation but had no effects on apoptosis in *Egln1*^{Tie2Cre} mice (Figures E5C and E5D). Expression of PAH-associated genes such as *Cav1*, *Bmpr2*, *IL6*, and *Cxcl12* was normalized in *Egln1*^{Tie2Cre} mouse lungs by C76 treatment (Figure E5E).

Given that severe PAH results in RV hypertrophy and failure (32), we next evaluated whether C76 treatment could inhibit RHF in *Egln1*^{Tie2Cre} mice. As shown in Figure 4A, severe RV hypertrophy seen in *Egln1*^{Tie2Cre} mice was markedly inhibited in C76-treated mice versus vehicle controls. Echocardiography showed that RV wall thickness and chamber size were markedly

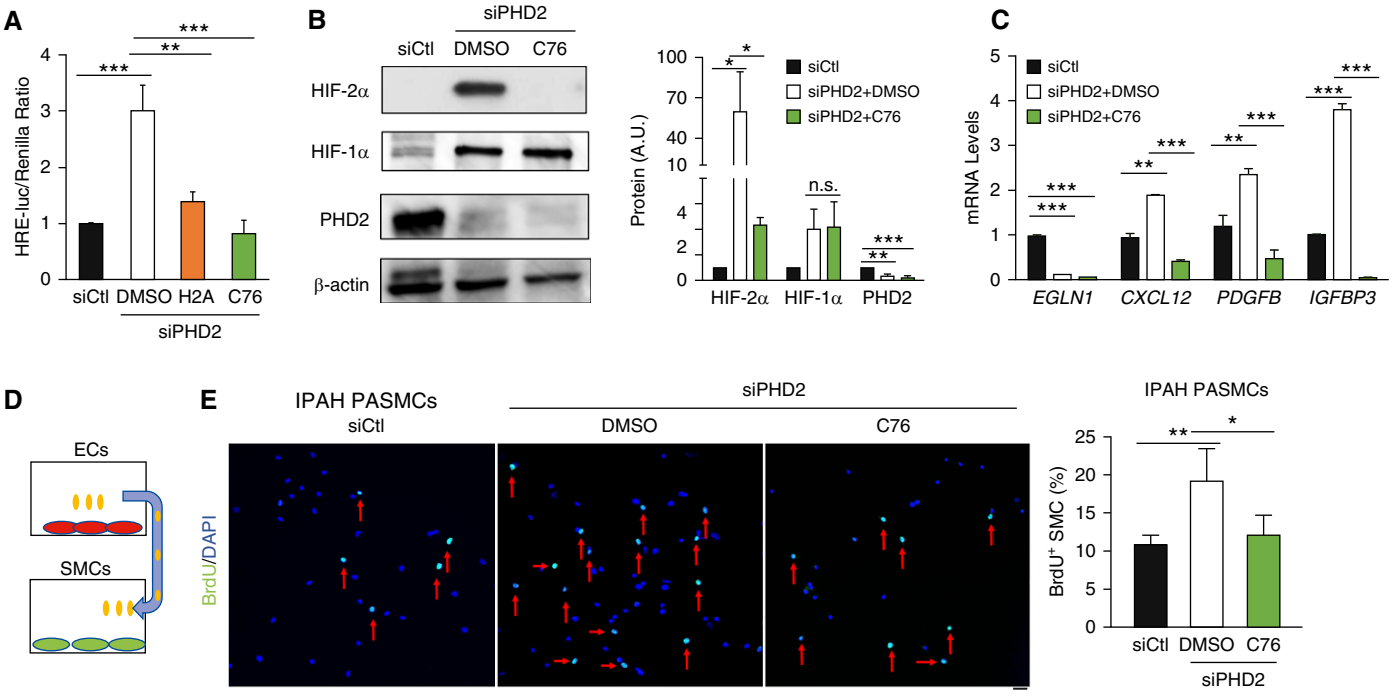

Figure 2. Inhibition of HIF-2α (hypoxia-inducible factor-2α) activation in human lung microvascular endothelial cells (HLMVECs) by treatment with HIF-2α inhibitors. (*A*) Luciferase assay showing that HIF-2α inhibitors (H2A [HIF-2α antagonist 2] and HIF-2α translational inhibitor compound 76 [C76]) suppressed HRE (hypoxia response element) activity induced by PHD2 (prolyl hydroxylase-2) deficiency in HLMVECs. HLMVECs were cotransfected with HRE-Luc plasmid and pRL-TK plasmid as well as PHD2 siRNA (siPHD2) or control scrambled RNA (siCtl). Six hours after transfection, the cells were treated with either H2A (20 μM), C76 (20 μM), or vehicle (DMSO) for another 14 hours and then lysed for luciferase assay. (*B*) Representative Western blot demonstrating that C76 treatment reduced HIF-2α protein levels but not HIF-1α protein levels in PHD2-deficient HLMVECs. (*C*) Quantitative RT-PCR analysis showing inhibited expression of HIF-2α target genes by C76 treatment in PHD2-deficient HLMVECs. (*D*) A diagram showing the strategy of smooth muscle cell (SMC) treatment with conditioned medium from ECs. (*E*) 5-Bromo-2′-deoxyuridine (BrdU) immunostaining demonstrating C76 inhibition of idiopathic pulmonary arterial hypertension (IPAH) pulmonary arterial SMC (PASMC) proliferation induced by conditioned medium from PHD2-deficient HLMVECs. Forty-eight hours after transfection with either PHD2 siRNA or control, HLMVECs were treated with DMSO or C76 (20 μM) for 24 hours in serum-free medium. Conditioned medium from these HLMVECs was then added to human PASMCs for 12 hours. After 12 hours of incubation with BrdU (10 μM), SMCs were fixed and immunostained with anti-BrdU (green) for quantification of cell proliferation. Red arrows indicate BrdU-positive cells. Sample size: (*A–C*) $n = 3$, (*E*) $n = 4$. $^{*}P < 0.05$, $^{**}P < 0.01$, and $^{***}P < 0.001$; n.s. = not significant. (*A–C* and *E*) One-way ANOVA with Tukey *post hoc* analysis. (*E*) Scale bar: 50 μm. A.U. = arbitrary units.

decreased with C76 treatment (Figures 4B, 4C, and E6A). RV fractional area change, indicative of RV contractility, was also drastically improved by C76 treatment (Figure 4D). Pathological examination revealed prominent interstitial and perivascular fibrosis in the RV of vehicle-treated *Egln1*^{Tie2Cre} mice, whereas C76 treatment markedly reduced RV fibrosis (Figures 4E and E6B). The reactivation of the embryonic gene program seen in heart failure (17, 33), including induced expression of skeletal α-actin, and atrial natriuretic factor was normalized in C76-treated *Egln1*^{Tie2Cre} mice compared with vehicle controls (Figure E6C). These data demonstrated that C76 treatment inhibited RV hypertrophy and failure. Accordingly, all C76-treated mice survived at the end of the 12-week study, whereas 40% of vehicle-treated mice had died within this time period (Figure 4F).

HIF-2α Inhibition Reverses Severe PAH and Right Heart Failure in SuHx Rats

Next we sought to determine whether inhibition of HIF-2α could reverse severe PAH in SuHx rats. Rats were administered a single dose of Sugen 5416 and kept in a hypoxia chamber for 3 weeks at 10% O_2, followed by 3 weeks of normoxia. These rats were then randomly assigned to two groups for treatment with vehicle or C76 for 3 weeks (Figure 5A). As shown in Figures E7A–E7C, expression of endothelial HIF-2α and its downstream target genes (also PH-associated genes) including *Edn1*, *Cxcl12*, and *Il6* was normalized in the lungs of C76-treated SuHx rats. C76 treatment markedly reduced RVSP compared with vehicle (Figure 5B), and normalized the PA AT/ET ratio, indicating normalization of PA diastolic function (Figure 5C).

Pulmonary vascular remodeling, including neointima formation, formation of occlusive lesions, and thickening of the PA wall (Figures 5D–5F), as well as muscularization of distal PAs (Figure E7D), was markedly inhibited in C76-treated rats compared with vehicle controls, which was likely due to decreased cell proliferation (Figure E7E). Together, these data demonstrate that C76 treatment reverses PAH in SuHx rats.

We then assessed the effect of C76 treatment on RV dysfunction in SuHx rats. C76 treatment markedly reduced RV hypertrophy, and RV wall thickness (Figures 6A and 6B), and improved RV contractility (Figure 6C) in SuHx rats. Fibrosis in the right ventricle was also markedly reduced by C76 treatment (Figure 6D). Thus, C76 inhibition of HIF-2α inhibited cardiac fibrosis and preserved RV function in SuHx rats.

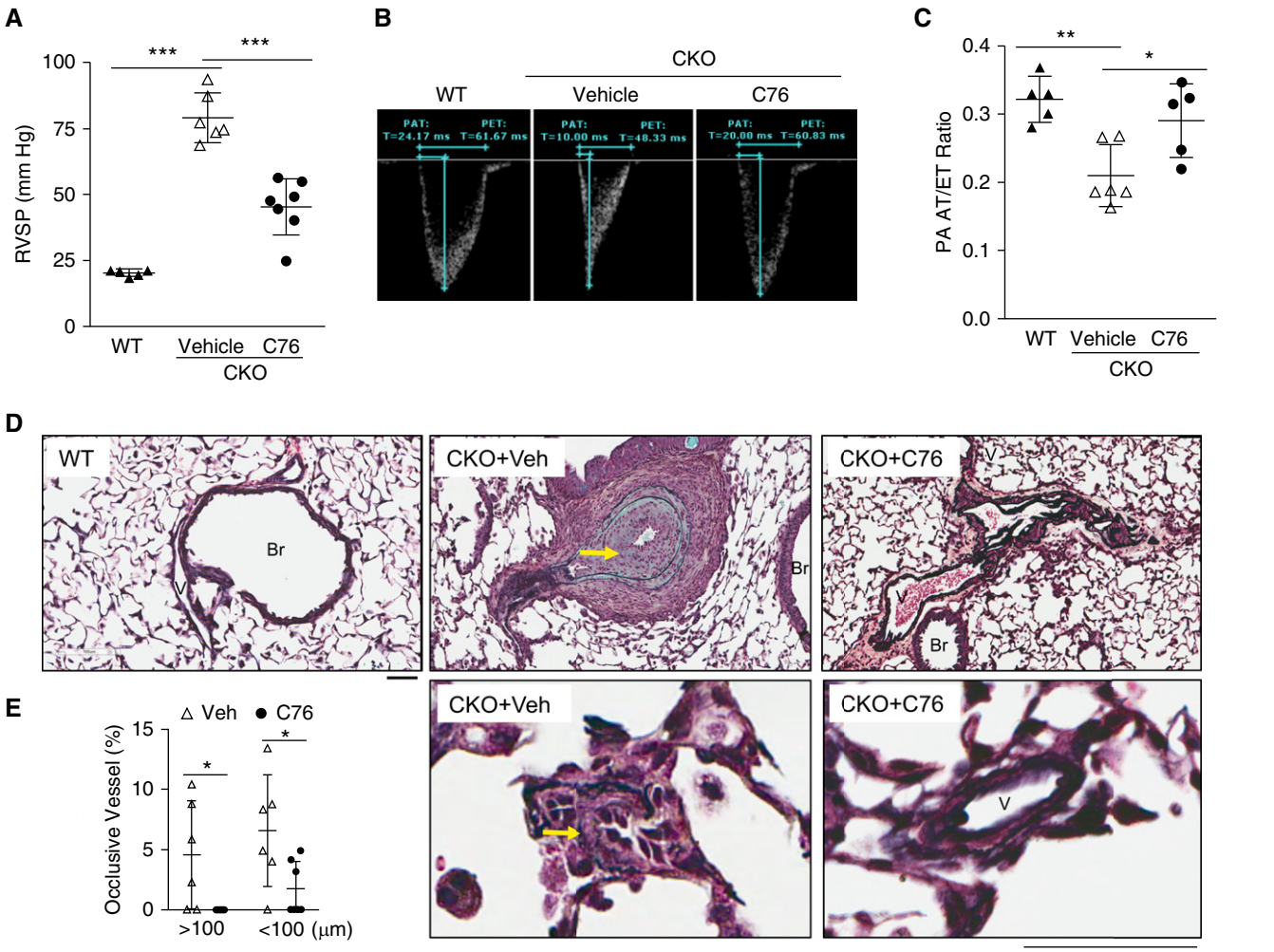

Figure 3. Pharmacological inhibition of HIF-2α (hypoxia-inducible factor-2α) inhibits severe pulmonary arterial hypertension (PAH) in *Egln1*^{Tie2Cre} mice. (*A*) Drastic decrease in right ventricular systolic pressure (RVSP) in C76 (compound 76)-treated *Egln1*^{Tie2Cre} (CKO) mice compared with vehicle-treated mice. Three-week-old *Egln1*^{Tie2Cre} mice exhibiting PAH were treated with either vehicle (0.5% DMSO) or C76 for 12 weeks. (*B* and *C*) Echocardiography measurement of pulmonary artery (PA) function showing normalization of PA acceleration time/ejection time (AT/ET) ratio in C76-treated *Egln1*^{Tie2Cre} mice. (*D*) Representative micrographs of Russell-Movat pentachrome staining, showing inhibited obliterative pulmonary vascular remodeling in C76-treated *Egln1*^{Tie2Cre} mice. Arrows indicate pulmonary vessels with severe remodeling. (*E*) Reduced occlusive lesions by C76 treatment in *Egln1*^{Tie2Cre} mice. Notably, there were no occlusive large vessels (>100 μm) in C76-treated *Egln1*^{Tie2Cre} mice. $^{*}P < 0.05$, $^{**}P < 0.01$, and $^{***}P < 0.001$. (*A* and *C*) One-way ANOVA with Tukey *post hoc* analysis for multiple group comparisons; and (*E*) Mann-Whitney test. (*D*) Scale bars: 50 μm. Br = bronchiole; V = vessel; Veh = vehicle; WT = wild type.

C76 Treatment Inhibits PAH in Monocrotaline-challenged Rats

We also examined the efficacy of C76 treatment in the MCT-induced rat PAH model. Two weeks after MCT challenge, the rats were treated with either C76 or vehicle for another 2 weeks (Figure 7A). Expression of endothelial HIF-2α and its downstream target genes was normalized or markedly inhibited in rats treated with C76 compared with vehicle (Figures E8A and E8B). C76 treatment inhibited PAH and RV hypertrophy, and restored PA function (Figures 7B, 7C, and E8C). Echocardiography also showed that C76 treatment decreased RV wall thickness (Figure E8D) and improved RV contractility (Figure 7D). Pulmonary vascular remodeling assessed by PA wall thickening, muscularization, and cell proliferation was also markedly attenuated by C76 treatment (Figures E8E and E8F). Remarkably, although all rats in the vehicle group had died by Day 28 after a lethal dose of MCT, C76 treatment resulted in a 70% survival rate at that time (Figure 7G). Taken together, these data demonstrate that targeting of HIF-2α reversed aberrant vascular remodeling and prevented right heart failure and death in the setting of severe PAH.

Discussion

The present study demonstrates that HIF-2α signaling is activated in pulmonary vascular ECs of patients with IPAH and that pharmacological inhibition of HIF-2α is a potential novel therapeutic approach for the effective treatment of PAH, thereby promoting survival. In *Egln1*^{Tie2Cre} mice, C76 treatment inhibited obliterative pulmonary vascular remodeling including neointima formation and occlusive vascular lesions, reduced RV hypertrophy and cardiac fibrosis, inhibited RVF, and promoted survival. In SuHx rats, C76

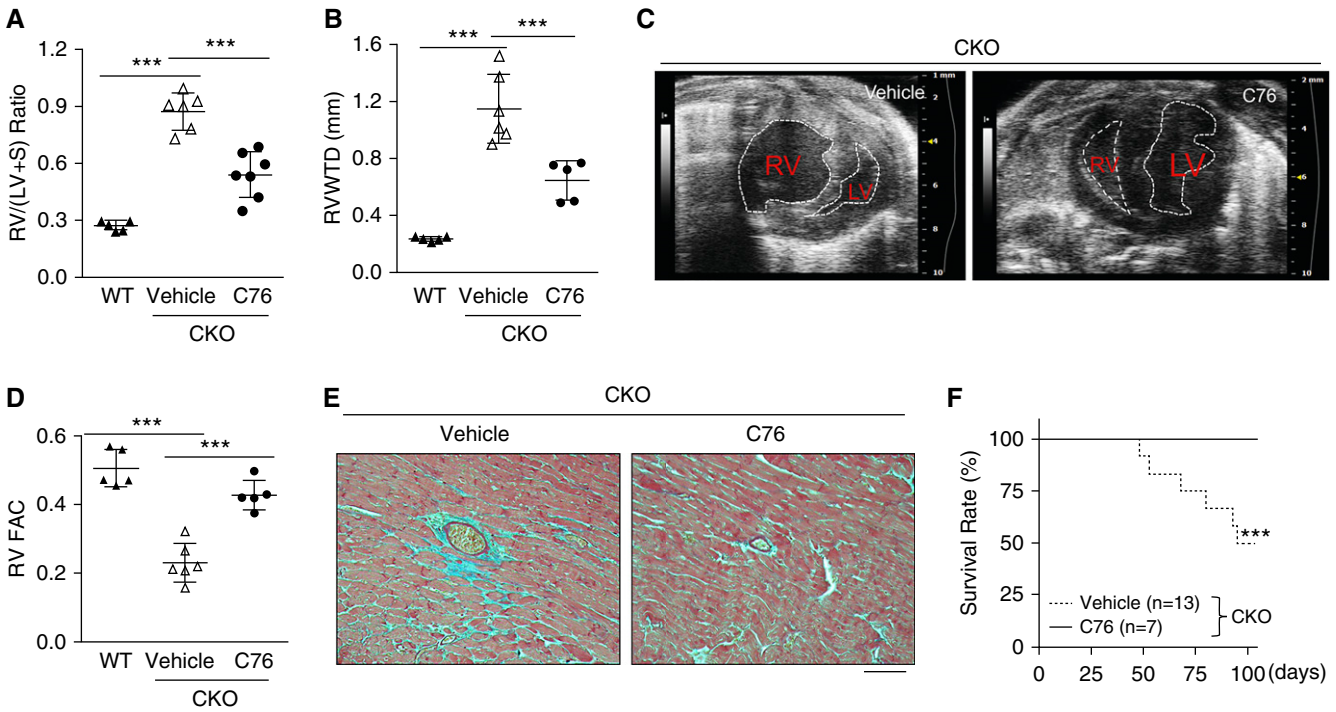

Figure 4. HIF-2α (hypoxia-inducible factor-2α) inhibition prevents right heart failure and cardiac fibrosis and promotes survival of *Egln1*^{Tie2Cre} mice. (*A*) Reduction in right ventricular (RV) hypertrophy by C76 (compound 76) treatment in *Egln1*^{Tie2Cre} (CKO) mice. (*B*) Quantification of transverse heart showing reduced RV wall thickness during diastole in C76-treated *Egln1*^{Tie2Cre} mice. (*C*) Representative M-mode echocardiography micrographs showing reduced RV chamber size in C76-treated *Egln1*^{Tie2Cre} mice compared with vehicle-treated CKO mice. The ventricular chambers are indicated with white lines. (*D*) Normalization of RV fractional area change, indicative of RV contractility, by C76 treatment in *Egln1*^{Tie2Cre} mice. (*E*) Representative micrographs of trichrome staining showing marked decrease in cardiac fibrosis in the right heart of a C76-treated *Egln1*^{Tie2Cre} mouse. Blue indicates collagen deposition. (*F*) C76 treatment promoted survival of *Egln1*^{Tie2Cre} mice. ***$P < 0.001$. (*A*, *B*, and *D*) One-way ANOVA with a Tukey *post hoc* analysis for multiple group comparisons; and (*F*) log-rank (Mantel-Cox) test. (*E*) Scale bar: 100 μm. LV = left ventricle; RV FAC = right ventricular fractional area change; RV/(LV + S) = ratio of right ventricle to left ventricle plus interventricular septum; RV WTD = RV wall thickness during diastole; WT = wild type.

treatment reversed pulmonary vascular remodeling, inhibited RV hypertrophy and cardiac fibrosis, and preserved cardiac function. Similarly, RVSP, pulmonary vascular remodeling, and RV hypertrophy as well as the mortality rate were markedly reduced in C76-treated MCT rats. The beneficial impact of inhibiting HIF-2α is particularly encouraging in a translational context, given that selective HIF-2α inhibitors have already been tested in phase 1 clinical trials in patients with renal cancer (34, 35).

The rodent models of PAH employed in our study represent a range of PAH-inducing stimuli and complement each other, and thereby provide important information about the translational potential of HIF-2α inhibition in the treatment of PAH. MCT-induced PAH in rats results from pulmonary accumulation of pyrrolic metabolites leading to endothelial injury and modest remodeling of the pulmonary vasculature (36, 37). SuHx-induced PAH in rats results from inhibition of the vascular endothelial growth factor (VEGF) receptors under hypoxic conditions, leading to the formation of plexiform lesions and neointima (28, 38). In the *Egln1*^{Tie2Cre} mouse model, PAH results from genetic deletion of PHD2 in endothelial and hematopoietic cells, culminating in severe vascular occlusion, the formation of plexiform-like lesions, RV hypertrophy and failure, and progressive mortality (17). Although any individual rodent model of PAH is unlikely to fully replicate the pathogenesis of human PAH, our study certainly demonstrates that HIF-2α inhibition reverses PAH in three mechanistically different rodent models of PAH.

Although endothelial deletion of HIF-2α induces minor PH in mice at late ages (39), studies highlight the crucial role of HIF-2α activation in the pathogenesis of PAH (14–19, 22), especially in regulating obliterative pulmonary vascular remodeling and RHF (17, 21, 22). The severe obliterative PAH phenotype seen in *Egln1*^{Tie2Cre} mice is dependent on HIF-2α activation (17, 22). Given that diminished expression of PHD2 is associated with occlusive vascular remodeling in patients with IPAH (17), targeting the abnormal PHD2/HIF-2α signaling is potentially clinically relevant. Consistently, other groups have shown that HIF-2α is upregulated in isolated PAECs and PA samples from patients with PAH (22, 40, 41). Here we observed marked activation of endothelial HIF-2α signaling in the lungs of three rodent models and also patients with IPAH, and provide clear evidence that targeting HIF-2α can reverse established PAH, inhibit vascular remodeling and RHF, and promote survival. Together, these studies strongly support the concept that selective targeting of HIF-2α is a potential therapeutic strategy for effective treatment of PAH and, importantly, for promoting survival.

HIF-2α controls the expression of many downstream targets that regulate vasoconstriction and vascular remodeling. We and other have demonstrated endothelial HIF-2α–dependent induction

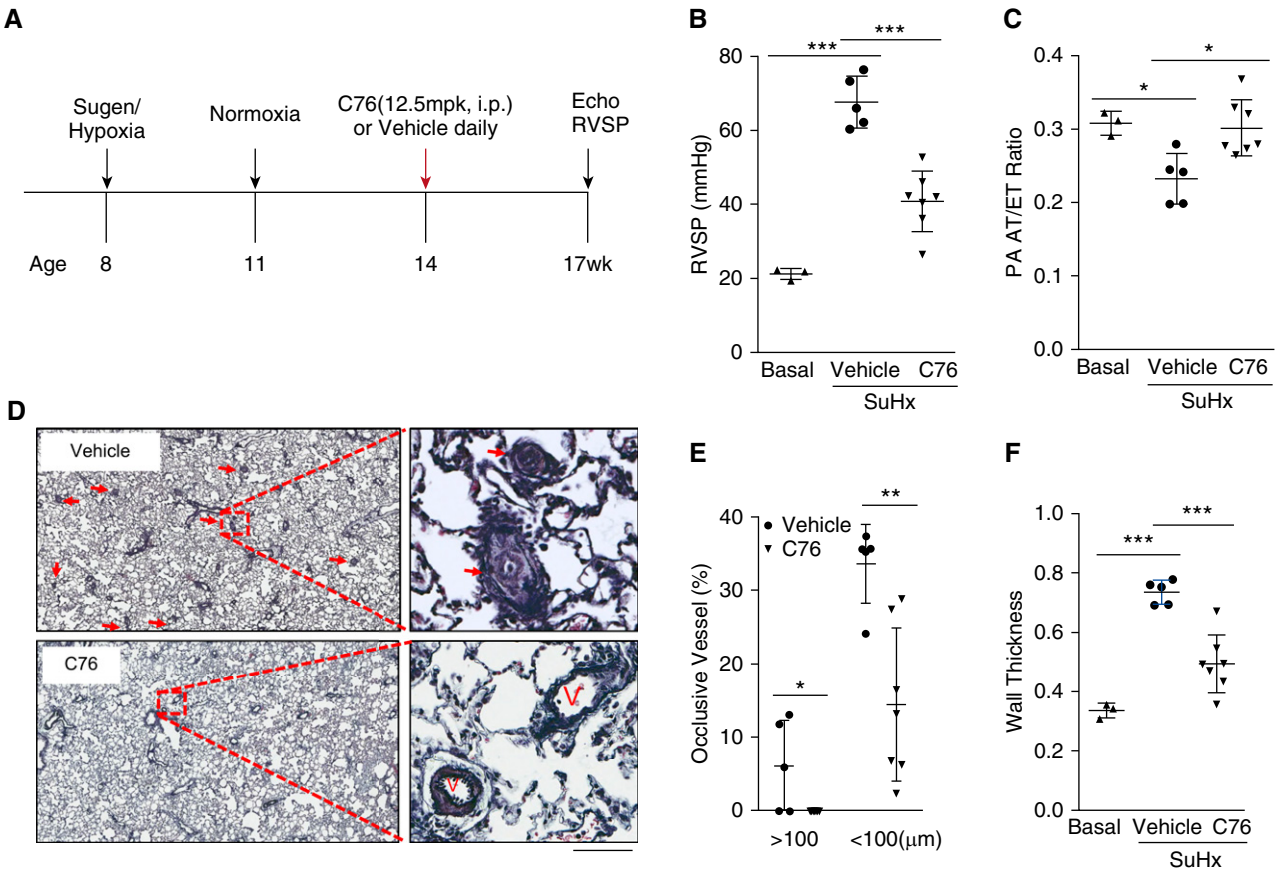

Figure 5. HIF-2α (hypoxia-inducible factor-2α) inhibition reverses severe pulmonary arterial hypertension in Sugen 5416/hypoxia (SuHx) rats. (*A*) Diagram showing the experimental timeline including C76 (compound 76) treatment in SuHx rats. (*B*) C76 treatment reduced right ventricular systolic pressure in SuHx rats. (*C*) Echocardiography measurements showing improvement in pulmonary artery (PA) diastolic function by C76 treatment in SuHx rats. (*D–F*) Representative images of Russell-Movat pentachrome staining (*D*) and vascular lesion quantification (*E* and *F*) demonstrating inhibited pulmonary vascular remodeling including reduction in occlusive lesions and PA wall thickness in C76-treated SuHx rats. Arrows point to pulmonary vessels with occlusive vascular remodeling. $^{*}P < 0.05$, $^{**}P < 0.01$, and $^{***}P < 0.001$. (*E*) Mann-Whitney test. (*B*, *C*, and *F*) One-way ANOVA with Tukey *post hoc* analysis for multiple group comparisons. (*D*) Scale bars: 200 μm. mpk = milligrams per kilogram; PA AT/ET = PA acceleration time/ejection time ratio; RVSP = right ventricular systolic pressure; V = vessel.

of the potent vasoconstrictor, endothelin-1 (*Edn1*), in the lungs of PHD2-deficient mice (17, 18). Cowburn and colleagues showed that increased endothelial arginase expression via HIF-2α activation disturbed normal nitric oxide homeostasis *in vivo*, which resulted in hypoxic pulmonary vasoconstriction (19). Thrombospondin-1, another HIF-2α target, was shown to increase fibroblast and SMC migration, recruit circulating monocytes, and contribute to hypoxic vascular remodeling and PAH (40, 42). Transgenic mice overexpressing IL-6, which is also a HIF-2α downstream target, exhibit occlusive vascular remodeling (43, 44). In addition, PHD2-deficient ECs induce PASMC proliferation through angiogenic paracrine factors including CXCL12, a specific HIF-2α target gene, in lung ECs (17, 45). Moreover, Tang and colleagues demonstrated that endothelial HIF-2α mediated endothelial mesenchymal transition via upregulation of downstream target SNAIL1/2 (22). Collectively, a broad dysregulation of multiple signaling pathways secondary to HIF-2α activation contributes to a progressive increase in pulmonary vascular resistance and severe pulmonary vascular remodeling in PAH. The protective impact of HIF-2α inhibition observed in our study could be attributed to normalized expression of these and other PAH-inducing genes such as *Il6*, *Cxcl12*, *Edn1*, *Cav1*, and *Bmpr2*. In other words, it is plausible that HIF-2α inhibitors could act through a number of different downstream targets of HIF-2α, which would otherwise facilitate the progression of PAH through parallel or divergent signaling pathways. Thus, targeting HIF-2α has great translational potential in reversing pulmonary vascular remodeling and normalizing vascular pulmonary homeostasis in PAH.

The HIF-2α inhibitor used in this study, C76, selectively decreases HIF-2α translation by enhancing the binding of IRP1 (iron-regulatory protein 1) to the 5′-untranslated region of *HIF2A*, but not *HIF1A* (31). Our *in vitro* and *in vivo* studies also demonstrate the selectivity of C76 in lung ECs. C76 treatment results in inhibition of HIF-2α expression but not HIF-1α in human lung ECs. We also observed *in vivo* inhibition of HIF-2α expression and its target genes in lungs from the three rodent PAH models. HIF-1α expression in lung ECs was not inhibited by C76 treatment in $Egln1^{Tie2Cre}$ mice. Thus,

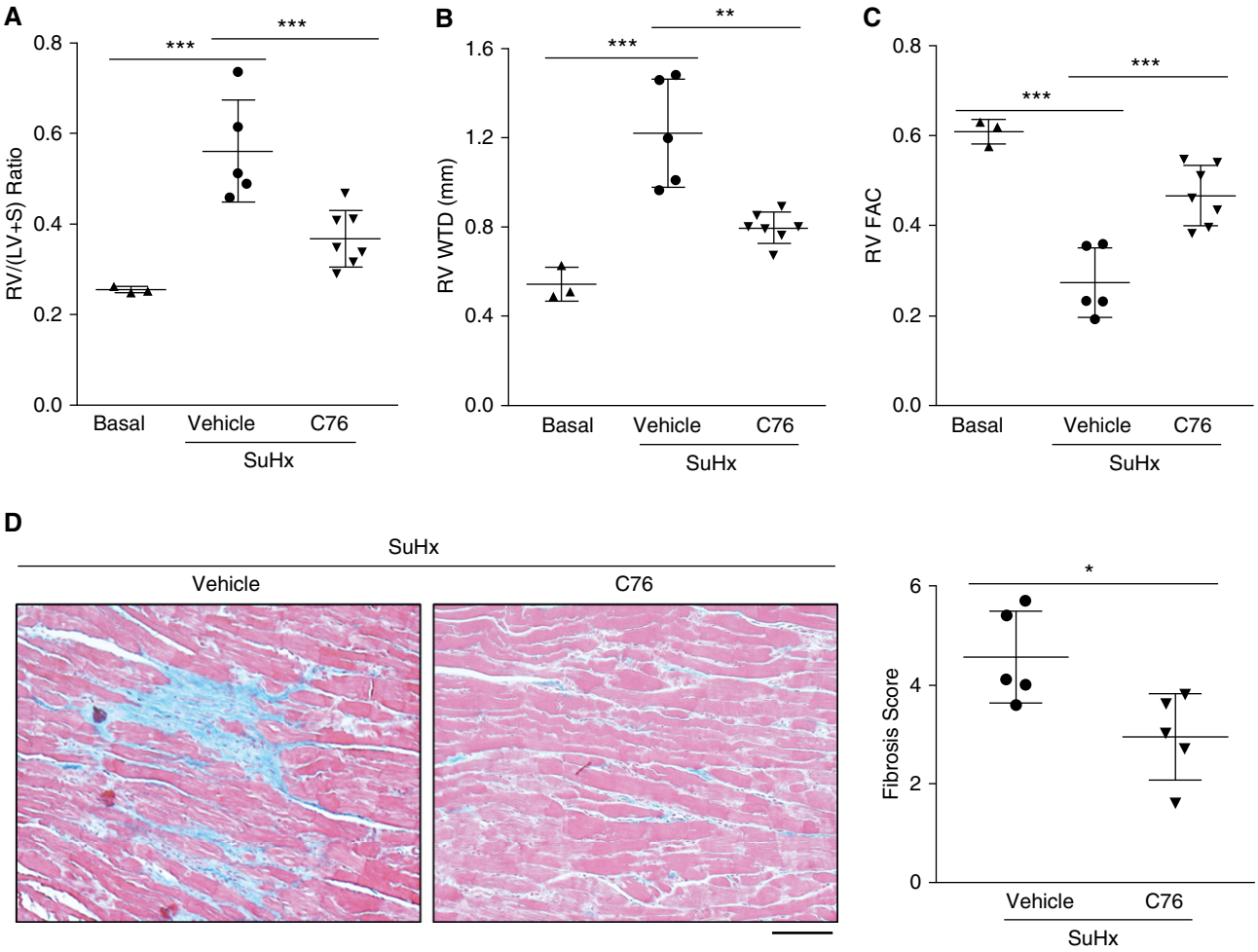

Figure 6. Treatment with a HIF-2α (hypoxia-inducible factor-2α) inhibitor prevents right heart failure and cardiac fibrosis in Sugen 5416/hypoxia (SuHx) rats. (*A*) C76 (compound 76) treatment inhibited right ventricular (RV) hypertrophy. (*B* and *C*) Echocardiography demonstrating decreased RV wall thickness (*B*) and restored RV contractility (*C*) in C76-treated SuHx rats. (*D*) Representative micrographs and quantification of trichrome staining demonstrating reduction in RV fibrosis by C76 treatment in SuHx rats. Blue indicates collagen deposition. $^{*}P < 0.05$, $^{**}P < 0.01$, and $^{***}P < 0.001$. (*A–C*) One-way ANOVA with Tukey *post hoc* analysis for multiple group comparisons. (*D*) Mann-Whitney test. (*D*) Scale bar: 50 μm. RV FAC = right ventricular fractional area change; RV/(LV + S) = ratio of right ventricle to left ventricle plus interventricular septum; RV WTD = RV wall thickness during diastole.

the *in vivo* effects of C76 in inhibiting PAH are likely attributable to selective HIF-2α targeting. In addition, other small molecules targeting HIF-2–ARNT (aryl hydrocarbon receptor nuclear translocator) heterodimerization have been developed, which have been tested in phase 1 clinical trials in patients with renal cancer (34, 35). It would be pertinent to determine whether this class of HIF-2α inhibitors also inhibits PAH.

As HIF-1α and HIF-2α share high sequence homology and similar O_2-dependent regulation, several compounds have been shown to inhibit the transcriptional activities of both HIF-1α and HIF-2α. Zhang and colleagues have reported that cardiac glycosides including digoxin inhibit both HIF-1α and HIF-2α protein synthesis but with lower inhibitory activity toward HIF-2α than HIF-1α (46). Acriflavine, a chromophore with antibacterial activities, was demonstrated to bind to the PAS-B domain of HIF-1α and HIF-2α and inhibit HIF dimerization and transcriptional activity (47). Both digoxin and acriflavine treatment limits RVSP elevation and RV hypertrophy in hypoxia-treated mice (48). Although these published studies indicate that HIF-1α inhibition mediates the *in vivo* effects, it is likely that HIF-2α inhibition by these compounds plays a determinant role in inhibiting PH.

In addition to ECs, HIF-2α is also expressed in alveolar epithelial cells and fibroblasts (49, 50). Although previous studies showed that both HIF-1α and HIF-2α inhibition on Postnatal Day 4 in mice impaired alveolar development, C76 treatment did not affect the mean linear intercept of alveoli in adult $Egln1^{Tie2Cre}$ mice (Figure E9A). Other report also showed that pulmonary fibroblast HIF-2α mediated hypoxia-induced fibroblast proliferation (50). It is likely that inhibited adventitial formation in C76-treated $Egln1^{Tie2Cre}$ mouse lungs is attributable to C76-inhibited fibroblast proliferation. Future studies are warranted to address this possibility. In addition, C76 may directly act on SMC HIF-2α and thereby inhibit pulmonary vascular remodeling. However, previous studies by Tang and colleagues demonstrated that $HIF2a^{Myh11Cre}$ mice were

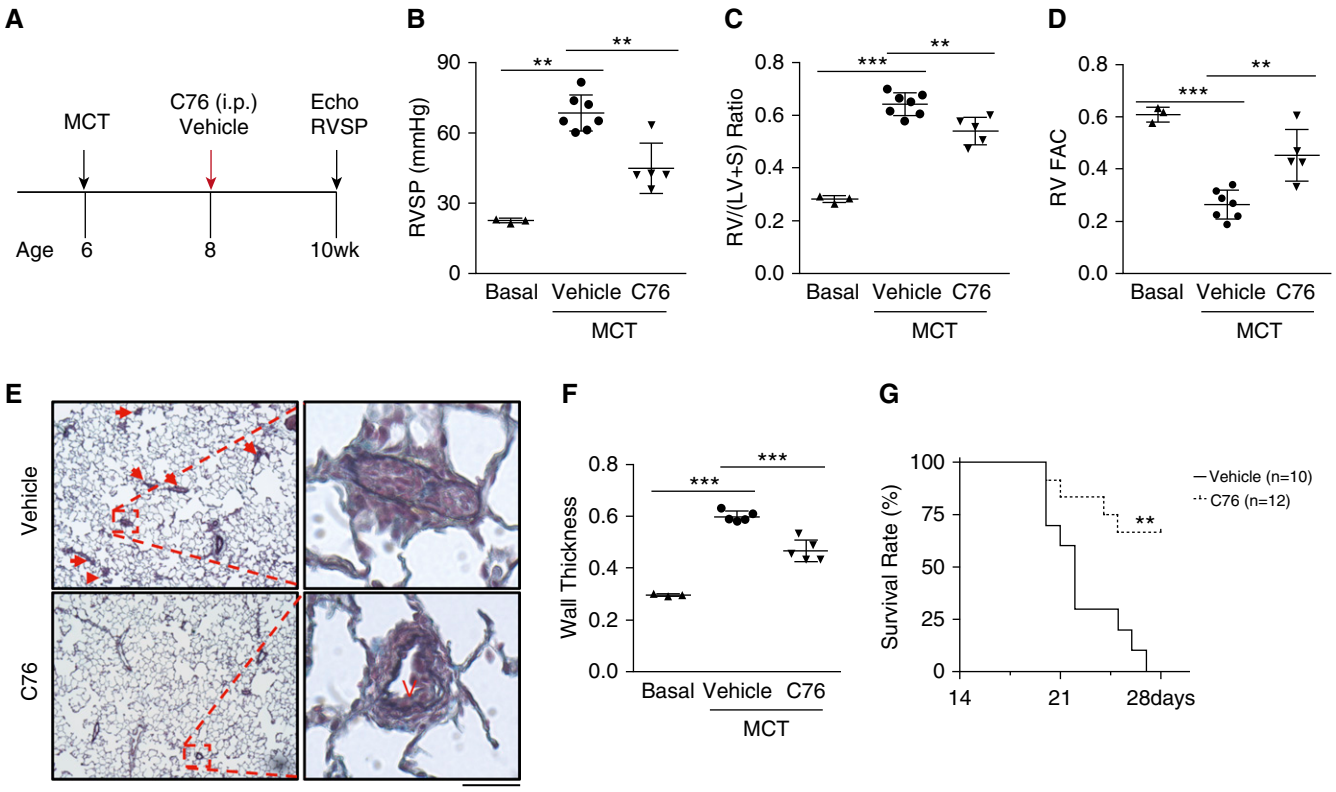

Figure 7. HIF-2α (hypoxia-inducible factor-2α) inhibition halts pulmonary arterial hypertension progression and promotes survival of monocrotaline (MCT) rats. (*A*) Diagram showing the experimental timeline for C76 (compound 76) treatment in MCT rats. (*B–D*) C76 treatment reduced right ventricular systolic pressure (*B*) and right ventricular (RV) hypertrophy (*C*) and normalized RV contractility (*D*). (*E*) Representative micrographs of Russell-Movat pentachrome staining of MCT rat lungs. Arrows indicate vascular lesions. (*F*) Quantification of pulmonary arterial wall thickness in MCT rat lungs. (*G*) Marked increase in survival of C76-treated MCT rats compared with vehicle controls. The rats were challenged with MCT at (*B–F*) 32 mg/kg or (*G*) 35 mg/kg. $^{**}P < 0.01$, $^{***}P < 0.001$. (*B–D* and *F*) One-way ANOVA with Tukey *post hoc* analysis for multiple group comparisons; and (*G*) log-rank (Mantel-Cox) test. (*E*) Scale bar: 50 μm. RV FAC = right ventricular fractional area change; RV/(LV + S) = ratio of right ventricle to left ventricle plus interventricular septum; RVSP = right ventricular systolic pressure; V = vessel.

not protected from hypoxia-induced PH, suggesting that SMC HIF-2α is not involved in the development of PH in mice (22). Our *Egln1*^{Tie2Cre}/*HIF2a*^{Tie2Cre} mice exhibited a normal pulmonary phenotype, demonstrating the importance of EC HIF-2α (17). Here we show that C76 did not affect the proliferation and apoptosis of PASMCs isolated from patients with IPAH (Figures E3D and E3E), indicating that C76 has no direct effects on SMCs. Importantly, C76 treatment did not affect heart rate, body weight, and plasma erythropoietin levels in both *Egln1*^{Tie2Cre} mice and SuHx-exposed rats (Figures E9B–E9D). These data suggest that targeting HIF-2α is potentially safe.

Collectively, our findings unveil the potential of targeting HIF-2α for effective treatment of PAH in patients and for promotion of survival, and provide convincing support for the development of novel and specific HIF-2α inhibitors that aim to reverse pulmonary vascular remodeling, inhibit RHF, and promote survival. ■

Author disclosures are available with the text of this article at www.atsjournals.org.

Acknowledgment: The authors thank Dr. John Wharton (Centre for Pharmacology and Therapeutics, Department of Medicine, Imperial College London, Hammersmith Hospital, London, UK) for providing lung tissue samples from patients with IPAH and unused donors. Data/tissue samples were provided by Pulmonary Hypertension Breakthrough Initiative (PHBI). Funding for the PHBI is provided under an NHLBI R24 grant (#R24HL123767) and by the Cardiovascular Medical Research and Education Fund.

References

1. McLaughlin VV, Archer SL, Badesch DB, Barst RJ, Farber HW, Lindner JR, *et al*.; ACCF/AHA. ACCF/AHA 2009 expert consensus document on pulmonary hypertension: a report of the American College of Cardiology Foundation Task Force on Expert Consensus Documents and the American Heart Association: developed in collaboration with the American College of Chest Physicians, American Thoracic Society, Inc., and the Pulmonary Hypertension Association. *Circulation* 2009;119:2250–2294.
2. Stacher E, Graham BB, Hunt JM, Gandjeva A, Groshong SD, McLaughlin VV, *et al*. Modern age pathology of pulmonary arterial hypertension. *Am J Respir Crit Care Med* 2012;186:261–272.
3. McLaughlin VV, Shah SJ, Souza R, Humbert M. Management of pulmonary arterial hypertension. *J Am Coll Cardiol* 2015;65:1976–1997.
4. Tuder RM, Stacher E, Robinson J, Kumar R, Graham BB. Pathology of pulmonary hypertension. *Clin Chest Med* 2013;34:639–650.

5. Pietra GG, Capron F, Stewart S, Leone O, Humbert M, Robbins IM, *et al*. Pathologic assessment of vasculopathies in pulmonary hypertension. *J Am Coll Cardiol* 2004;43(12, Suppl. S):25S–32S.
6. Rabinovitch M. Pathobiology of pulmonary hypertension. *Annu Rev Pathol* 2007;2:369–399.
7. Thompson AAR, Lawrie A. Targeting vascular remodeling to treat pulmonary arterial hypertension. *Trends Mol Med* 2017;23: 31–45.
8. Lau EMT, Giannoulatou E, Celermajer DS, Humbert M. Epidemiology and treatment of pulmonary arterial hypertension. *Nat Rev Cardiol* 2017;14:603–614.
9. Semenza GL. Hypoxia-inducible factors in physiology and medicine. *Cell* 2012;148:399–408.
10. Shimoda LA, Semenza GL. HIF and the lung: role of hypoxia-inducible factors in pulmonary development and disease. *Am J Respir Crit Care Med* 2011;183:152–156.
11. Yu AY, Shimoda LA, Iyer NV, Huso DL, Sun X, McWilliams R, *et al*. Impaired physiological responses to chronic hypoxia in mice partially deficient for hypoxia-inducible factor 1α. *J Clin Invest* 1999;103: 691–696.
12. Brusselmans K, Compernolle V, Tjwa M, Wiesener MS, Maxwell PH, Collen D, *et al*. Heterozygous deficiency of hypoxia-inducible factor-2α protects mice against pulmonary hypertension and right ventricular dysfunction during prolonged hypoxia. *J Clin Invest* 2003; 111:1519–1527.
13. Ball MK, Waypa GB, Mungai PT, Nielsen JM, Czech L, Dudley VJ, *et al*. Regulation of hypoxia-induced pulmonary hypertension by vascular smooth muscle hypoxia-inducible factor-1α. *Am J Respir Crit Care Med* 2014;189:314–324.
14. Gale DP, Harten SK, Reid CD, Tuddenham EG, Maxwell PH. Autosomal dominant erythrocytosis and pulmonary arterial hypertension associated with an activating HIF2α mutation. *Blood* 2008;112: 919–921.
15. Tan Q, Kerestes H, Percy MJ, Pietrofesa R, Chen L, Khurana TS, *et al*. Erythrocytosis and pulmonary hypertension in a mouse model of human *HIF2A* gain of function mutation. *J Biol Chem* 2013;288: 17134–17144.
16. Hickey MM, Richardson T, Wang T, Mosqueira M, Arguiri E, Yu H, *et al*. The von Hippel-Lindau Chuvash mutation promotes pulmonary hypertension and fibrosis in mice. *J Clin Invest* 2010;120: 827–839.
17. Dai Z, Li M, Wharton J, Zhu MM, Zhao YY. Prolyl-4 hydroxylase 2 (PHD2) deficiency in endothelial cells and hematopoietic cells induces obliterative vascular remodeling and severe pulmonary arterial hypertension in mice and humans through hypoxia-inducible factor-2α. *Circulation* 2016;133:2447–2458.
18. Kapitsinou PP, Rajendran G, Astleford L, Michael M, Schonfeld MP, Fields T, *et al*. The endothelial prolyl-4-hydroxylase domain 2/hypoxia-inducible factor 2 axis regulates pulmonary artery pressure in mice. *Mol Cell Biol* 2016;36:1584–1594.
19. Cowburn AS, Crosby A, Macias D, Branco C, Colaço RD, Southwood M, *et al*. HIF2α-arginase axis is essential for the development of pulmonary hypertension. *Proc Natl Acad Sci USA* 2016;113: 8801–8806.
20. Smith TG, Brooks JT, Balanos GM, Lappin TR, Layton DM, Leedham DL, *et al*. Mutation of von Hippel-Lindau tumour suppressor and human cardiopulmonary physiology. *PLoS Med* 2006;3: e290.
21. Dai Z, Zhao YY. Discovery of a murine model of clinical PAH: mission impossible? *Trends Cardiovasc Med* 2017;27:229–236.
22. Tang H, Babicheva A, McDermott KM, Gu Y, Ayon RJ, Song S, *et al*. Endothelial HIF-2α contributes to severe pulmonary hypertension due to endothelial-to-mesenchymal transition. *Am J Physiol Lung Cell Mol Physiol* 2018;314:L256–L275.
23. Dai Z, Zhu MM, Zhao Y. Target vascular remodeling and right heart failure with selective hypoxia inducible factor-2α inhibitors [abstract 13871]. *Circulation* 2017;136(Suppl. 1):A13871.
24. Dai Z, Zhu MM, Zhang X, Tarjus A, Zhao Y. Selective targeting HIF-2α for treatment of pulmonary arterial hypertension [abstract 1016.6]. *FASEB J* 2017;31 (Suppl. 1):1016.6.
25. Zhao YY, Zhao YD, Mirza MK, Huang JH, Potula HH, Vogel SM, *et al*. Persistent eNOS activation secondary to caveolin-1 deficiency induces pulmonary hypertension in mice and humans through PKG nitration. *J Clin Invest* 2009;119:2009–2018.
26. Dai Z, Zhu MM, Peng Y, Jin H, Machireddy N, Qian Z, *et al*. Endothelial and smooth muscle cell interaction via FoxM1 signaling mediates vascular remodeling and pulmonary hypertension. *Am J Respir Crit Care Med* 2018;198:788–802.
27. Zhao YD, Cai L, Mirza MK, Huang X, Geenen DL, Hofmann F, *et al*. Protein kinase G-I deficiency induces pulmonary hypertension through Rho A/Rho kinase activation. *Am J Pathol* 2012;180: 2268–2275.
28. Taraseviciene-Stewart L, Kasahara Y, Alger L, Hirth P, Mc Mahon G, Waltenberger J, *et al*. Inhibition of the VEGF receptor 2 combined with chronic hypoxia causes cell death–dependent pulmonary endothelial cell proliferation and severe pulmonary hypertension. *FASEB J* 2001;15:427–438.
29. Stenmark KR, Meyrick B, Galie N, Mooi WJ, McMurtry IF. Animal models of pulmonary arterial hypertension: the hope for etiological discovery and pharmacological cure. *Am J Physiol Lung Cell Mol Physiol* 2009;297:L1013–L1032.
30. Scheuermann TH, Li Q, Ma HW, Key J, Zhang L, Chen R, *et al*. Allosteric inhibition of hypoxia inducible factor-2 with small molecules. *Nat Chem Biol* 2013;9:271–276.
31. Zimmer M, Ebert BL, Neil C, Brenner K, Papaioannou I, Melas A, *et al*. Small-molecule inhibitors of HIF-2α translation link its 5′UTR iron-responsive element to oxygen sensing. *Mol Cell* 2008;32: 838–848.
32. Ryan JJ, Archer SL. The right ventricle in pulmonary arterial hypertension: disorders of metabolism, angiogenesis and adrenergic signaling in right ventricular failure. *Circ Res* 2014;115:176–188.
33. Zhao YY, Liu Y, Stan RV, Fan L, Gu Y, Dalton N, *et al*. Defects in caveolin-1 cause dilated cardiomyopathy and pulmonary hypertension in knockout mice. *Proc Natl Acad Sci USA* 2002;99: 11375–11380.
34. Chen W, Hill H, Christie A, Kim MS, Holloman E, Pavia-Jimenez A, *et al*. Targeting renal cell carcinoma with a HIF-2 antagonist. *Nature* 2016; 539:112–117.
35. Cho H, Du X, Rizzi JP, Liberzon E, Chakraborty AA, Gao W, *et al*. On-target efficacy of a HIF-2α antagonist in preclinical kidney cancer models. *Nature* 2016;539:107–111.
36. Lalich JJ, Merkow L. Pulmonary arteritis produced in rat by feeding *Crotalaria spectabilis*. *Lab Invest* 1961;10:744–750.
37. Kay JM, Harris P, Heath D. Pulmonary hypertension produced in rats by ingestion of *Crotalaria spectabilis* seeds. *Thorax* 1967;22:176–179.
38. Abe K, Toba M, Alzoubi A, Ito M, Fagan KA, Cool CD, *et al*. Formation of plexiform lesions in experimental severe pulmonary arterial hypertension. *Circulation* 2010;121:2747–2754.
39. Skuli N, Liu L, Runge A, Wang T, Yuan L, Patel S, *et al*. Endothelial deletion of hypoxia-inducible factor-2α (HIF-2α) alters vascular function and tumor angiogenesis. *Blood* 2009;114:469–477.
40. Labrousse-Arias D, Castillo-González R, Rogers NM, Torres-Capelli M, Barreira B, Aragonés J, *et al*. HIF-2α–mediated induction of pulmonary thrombospondin-1 contributes to hypoxia-driven vascular remodelling and vasoconstriction. *Cardiovasc Res* 2016; 109:115–130.
41. Barnes EA, Chen CH, Sedan O, Cornfield DN. Loss of smooth muscle cell hypoxia inducible factor-1α underlies increased vascular contractility in pulmonary hypertension. *FASEB J* 2017;31: 650–662.
42. Kumar R, Mickael C, Kassa B, Gebreab L, Robinson JC, Koyanagi DE, *et al*. TGF-β activation by bone marrow–derived thrombospondin-1 causes *Schistosoma*- and hypoxia-induced pulmonary hypertension. *Nat Commun* 2017;8:15494.
43. Steiner MK, Syrkina OL, Kolliputi N, Mark EJ, Hales CA, Waxman AB. Interleukin-6 overexpression induces pulmonary hypertension. *Circ Res* 2009;104:236–244, 28p followng 244.
44. Ryu JH, Yang S, Shin Y, Rhee J, Chun CH, Chun JS. Interleukin-6 plays an essential role in hypoxia-inducible factor 2α–induced experimental osteoarthritic cartilage destruction in mice. *Arthritis Rheum* 2011;63: 2732–2743.

45. Martin SK, Diamond P, Williams SA, To LB, Peet DJ, Fujii N, *et al*. Hypoxia-inducible factor-2 is a novel regulator of aberrant CXCL12 expression in multiple myeloma plasma cells. *Haematologica* 2010; 95:776–784.
46. Zhang H, Qian DZ, Tan YS, Lee K, Gao P, Ren YR, *et al*. Digoxin and other cardiac glycosides inhibit HIF-1α synthesis and block tumor growth. *Proc Natl Acad Sci USA* 2008;105:19579–19586.
47. Lee K, Zhang H, Qian DZ, Rey S, Liu JO, Semenza GL. Acriflavine inhibits HIF-1 dimerization, tumor growth, and vascularization. *Proc Natl Acad Sci USA* 2009;106:17910–17915.
48. Abud EM, Maylor J, Undem C, Punjabi A, Zaiman AL, Myers AC, *et al*. Digoxin inhibits development of hypoxic pulmonary hypertension in mice. *Proc Natl Acad Sci USA* 2012;109:1239–1244.
49. Compernolle V, Brusselmans K, Acker T, Hoet P, Tjwa M, Beck H, *et al*. Loss of HIF-2α and inhibition of VEGF impair fetal lung maturation, whereas treatment with VEGF prevents fatal respiratory distress in premature mice. *Nat Med* 2002;8:702–710.
50. Eul B, Rose F, Krick S, Savai R, Goyal P, Klepetko W, *et al*. Impact of HIF-1α and HIF-2α on proliferation and migration of human pulmonary artery fibroblasts in hypoxia. *FASEB J* 2006;20:163–165.